ARMY RESEARCH LABORATORY

Effective Three-Dimensional (3-D) Finite Element Material Stiffness Formulation for Modeling Laminated Composites

A. Alexander
CUSTOM ANALYTICAL ENGINEERING SYSTEM, INC.

J. T. Tzeng
W. H. Drysdale
B. P. Burns
U.S. ARMY RESEARCH LABORATORY

ARL-TR-1051 April 1996

NOTICES

Destroy this report when it is no longer needed. DO NOT return it to the originator.

Additional copies of this report may be obtained from the National Technical Information Service, U.S. Department of Commerce, 5285 Port Royal Road, Springfield, VA 22161.

The findings of this report are not to be construed as an official Department of the Army position, unless so designated by other authorized documents.

The use of trade names or manufacturers' names in this report does not constitute indorsement of any commercial product.

REPORT DOCUMENTATION PAGE

Form Approved
OMB No. 0704-0188

1. AGENCY USE ONLY *(Leave blank)*	2. REPORT DATE	3. REPORT TYPE AND DATES COVERED
	April 1996	Final, October 1990 - September 1993

4. TITLE AND SUBTITLE
Effective Three-Dimensional (3-D) Finite Element Material Stiffness Formulation for Modeling Laminated Composites

5. FUNDING NUMBERS
PR: 1L162618AH80

6. AUTHOR(S)
A. Alexander*, J. T. Tzeng, W. H. Drysdale, and B. P. Burns

7. PERFORMING ORGANIZATION NAME(S) AND ADDRESS(ES)
U.S. Army Research Laboratory
ATTN: AMSRL-WT-PD
Aberdeen Proving Ground, MD 21005-5066

8. PERFORMING ORGANIZATION REPORT NUMBER
ARL-TR-1051

9. SPONSORING/MONITORING AGENCY NAMES(S) AND ADDRESS(ES)

10.SPONSORING/MONITORING AGENCY REPORT NUMBER

11. SUPPLEMENTARY NOTES
* Custom Analytical Engineering System, Inc., Flintstone, MD 21530.

12a. DISTRIBUTION/AVAILABILITY STATEMENT
Approved for public release; distribution is unlimited.

12b. DISTRIBUTION CODE

13. ABSTRACT *(Maximum 200 words)*

A model has been developed to compute the effective properties for an element with arbitrarily shaped composite material regions. The analysis utilizes the strain energy approach and finite element technique to resolve the complexity of three-dimensional (3-D) layer geometry, anistropy, ply orientations, and multi-material regions within an element. Accordingly, the model accounts for the complex element geometries resulting from material discontinuity, changes in mesh density, and arbitrarily shaped elements that cannot be readily aligned with the layers of the laminate.

The computed elastic constants are accurate, especially for the transverse shear properties. The analysis is particularly suitable for finite element applications of near-net shaped, thick-section structures. Based on the model, a pre- and postprocessor was developed to generate finite element models for computer codes such as DYNA3D and ABAQUS. Results from the finite element analysis can also be recovered to ply-by-ply basis stresses and strains.

14. SUBJECT TERMS
composite, effective properties, finite element, structural analysis, shear properties, conformal mapping

15. NUMBER OF PAGES
42

16. PRICE CODE

17. SECURITY CLASSIFICATION OF REPORT	18. SECURITY CLASSIFICATION OF THIS PAGE	19. SECURITY CLASSIFICATION OF ABSTRACT	20. LIMITATION OF ABSTRACT
UNCLASSIFIED	UNCLASSIFIED	UNCLASSIFIED	UL

INTENTIONALLY LEFT BLANK.

TABLE OF CONTENTS

INTENTIONALLY LEFT BLANK.

LIST OF FIGURES

LIST OF TABLES

INTENTIONALLY LEFT BLANK.

1. INTRODUCTION

Composite material offers a great potential and flexibility in structural design because of the anisotropy of material properties, unique ply-by-ply constructions, and novel fabrication methods. To extract the maximum performance, structures, in general, are designed with various ply orientations and stacking sequence from layer to layer within the structures. This flexibility does enhance the structural design; however, it also increases the degree of difficulty for analysis, particularly by using the finite element method (FEM). This is especially true for a thick-section composite structure, which may consist of thousands of anisotropic layers.

There are two analytical approaches that can be used for analysis of composite structures by FEM, a layer-by-layer analysis or a property smearing model. The layer-by-layer analysis approach will, in general, result in a huge finite element model with thousands of elements required to maintain a proper aspect ratio of elements. Therefore, a tremendous computational effort is required, especially for a dynamic analysis. For a thick-section large composite structure, the layer-by-layer approach is not practical.

Another approach is to use the smeared (effective) properties for the elements. Accordingly, each element consists of several layers and material blocks. The properties of elements are calculated from the properties of the contained layers based on certain assumptions. The effective properties of the input model are crucial to the accuracy of FEM analysis. Several models based on either "laminated plate theory" or "rule of mixture" have been developed to compute the effective properties for use for FEM analysis. However, these approaches cannot be used to calculate the effective properties accurately for a very common element with irregular geometry. For example, a taper-shaped element from a filament-wound cone model is illustrated in Figure 1.

Enie and Rizzo (1970), Pagano (1974), and Christensen and Zywicz (1989) derived the effective properties from laminated plate theory. Particularly, Pagano's model is an exact three-dimensional (3-D) solution calculated from a laminated plate. These models were all developed by assuming a finite thickness in the transverse direction (2-D geometry). In general, a constant interlaminar shear stress distribution through the thickness is assumed for these models. Properties calculated from these models may be suitable for thin-shell structures, but are not proper for a thick structure or a block element since these models do not correctly account for the properties in the transverse direction, especially for the transverse shear and shear coupling properties. In addition, the plate theory is limited to a rectangular geometry and can never be used for an arbitrarily shaped geometry which commonly occurs in FEM modeling.

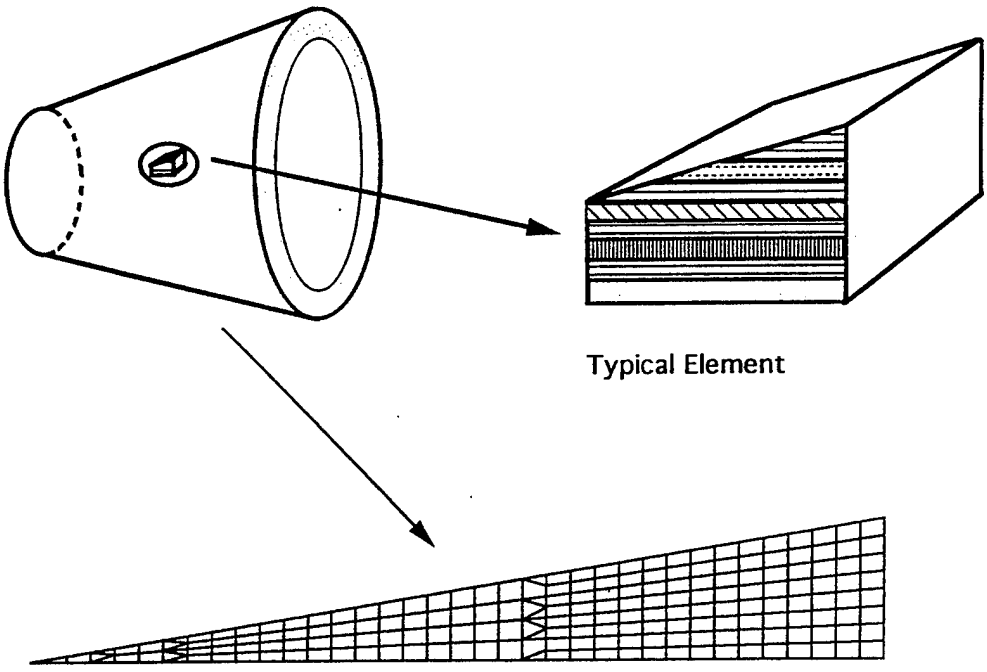

Figure 1. Taper-shaped elements in an FEM cone model.

Models developed by Chou, Carleone, and Hsu (1971) and Sun and Li (1988) assumed a uniform displacement in the planes parallel to the laminate and a uniform stress in the transverse direction of the plane. The transverse (interlaminar) shear components are calculated on the basis of volume average. The in-plane properties resulting from this approach are correct. However, the transverse shear properties are not accurate enough and, thus, not suitable, for thick-section structures, which generally have large transverse shear deformations.

One of the common shortcomings of these models is the limitation of geometry. The laminate is generally restricted to uniform thickness flat plate or thin shell configurations with layers aligned along element boundaries. Element faces must be rectangular in both the plane of the laminate and the through-thickness directions. This limitation makes it very difficult to model regions containing ply drop-offs, or layer terminations, and impose restrictions on the capability to generate finite element meshes for complex geometries that require changes in mesh density and/or arbitrarily shaped elements that cannot be readily aligned with the layers of the laminate.

Figure 2 shows a generalized case of an element in a region containing several materials. The effective properties of the element certainly cannot be calculated correctly with any of the models

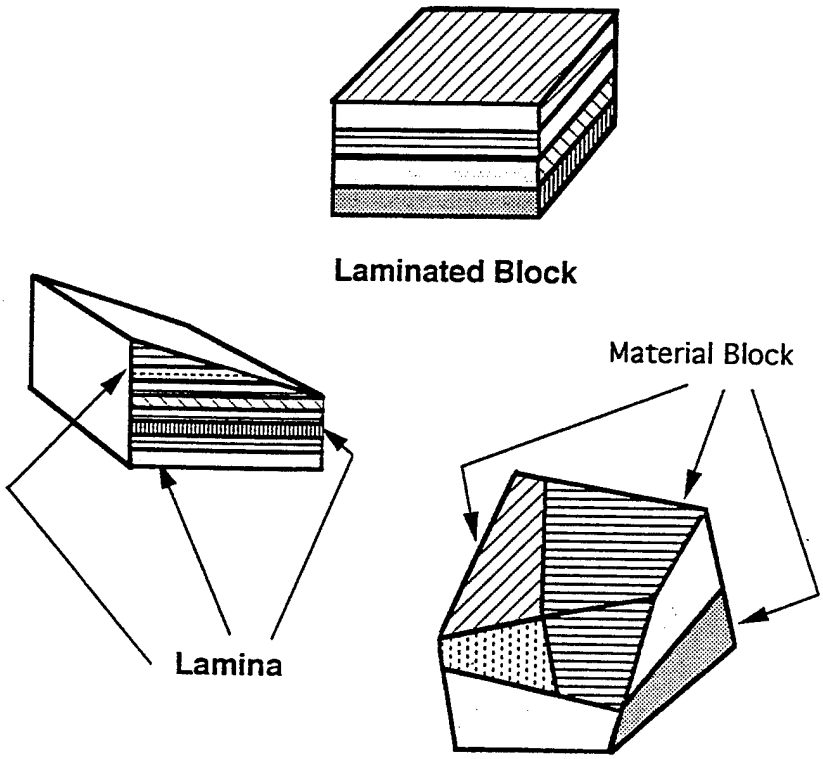

Figure 2. Arbitrarily shaped element with multiple anisotropic layers and materials.

mentioned previously. Commercial packages typically use the volume average approach for computing effective properties in elements such as this, leading to potential inaccuracies in results, especially for irregular shaped elements. Accordingly, there is a strong need to develop an accurate property model for FEM applications.

The objective of this investigation is to develop a model that provides accurate 3-D effective properties for arbitrarily shaped solid continuum elements containing multiple layers and materials with various orientations and shapes. The second objective will be to develop a pre-processor incorporating the effective property model in generating accurate finite element representations of 3-D laminated material structures for ABAQUS and DYNA3D.

2. MODEL DEVELOPMENT

Consider a portion of a material block contained within some internal region of an element's volume. Relative to the global frame with coordinates (x^1, x^2, x^3) illustrated in Figure 3, the generalized elastic constitutive behavior of each material block is described by the relations

$$t_i^j = C_{ik}^{jl}\, \varepsilon_l^k ,$$

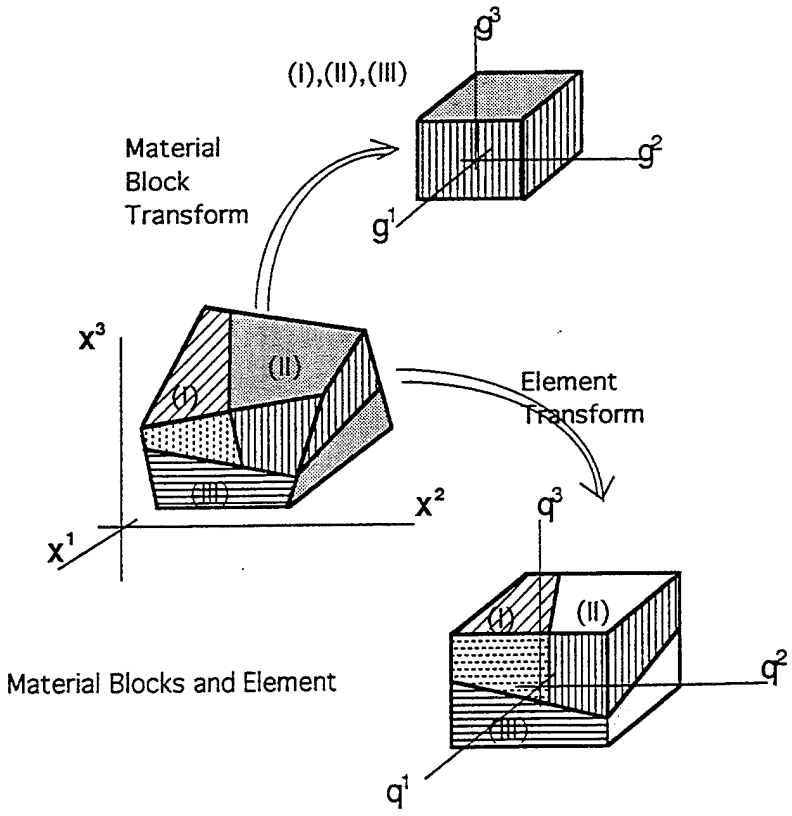

Figure 3. Coordinates transforms of material blocks and elements.

where t_i^j is the stress tensor, ε_l^k is the strain tensor, and C_{ik}^{jl} represents the material stiffness tensor relative to the global frame.

We assume the deformation field within the volume portion contained in the element bounds is continuous such that it can be approximated as a function of the displacements at the corner points that bound the volume portion.

We first incorporate the transformation of global coordinates to isoparametric coordinates within the volume portion

$$x^i = N^\alpha X_\alpha^i, \tag{1}$$

where the X_α^i are the global coordinates of the corner points.

The notation used herein follows the standard summation convention for repeated indices. English indices correspond to the range (1,2,3), referring to the three independent spacial components of a variable while Greek indices correspond to the (1,2,...Γ) discrete point values and $N^{\alpha}(g^1, g^2, g^3)$ isoparametric interpolation functions used for describing the continuous variation of a parameter within a volume. The interpolation functions, written in terms of the isoparametric coordinates g^i of the volume, are expressed as:

Linear formulation (Γ=8):

$$N^1=\frac{1}{8}(1-g^1)\,(1-g^2)\,(1-g^3) \qquad N^5=\frac{1}{8}(1-g^1)\,(1-g^2)\,(1+g^3)$$
$$N^2=\frac{1}{8}(1+g^1)\,(1-g^2)\,(1-g^3) \qquad N^6=\frac{1}{8}(1+g^1)\,(1-g^2)\,(1+g^3)$$
$$N^3=\frac{1}{8}(1+g^1)\,(1+g^2)\,(1-g^3) \qquad N^7=\frac{1}{8}(1+g^1)\,(1+g^2)\,(1+g^3)$$
$$N^4=\frac{1}{8}(1-g^1)\,(1+g^2)\,(1-g^3) \qquad N^8=\frac{1}{8}(1-g^1)\,(1+g^2)\,(1+g^3)$$

Quadratic formulation (Γ=20):

$$N^1=-\frac{1}{8}(1-g^1)\,(1-g^2)\,(1-g^3)\,(2+g^1+g^2+g^3)$$
$$N^2=-\frac{1}{8}(1+g^1)\,(1-g^2)\,(1-g^3)\,(2-g^1+g^2+g^3)$$
$$N^3=-\frac{1}{8}(1+g^1)\,(1+g^2)\,(1-g^3)\,(2-g^1-g^2+g^3)$$
$$N^4=-\frac{1}{8}(1-g^1)\,(1+g^2)\,(1-g^3)\,(2+g^1-g^2+g^3)$$
$$N^5=-\frac{1}{8}(1-g^1)\,(1-g^2)\,(1+g^3)\,(2+g^1+g^2-g^3)$$
$$N^6=-\frac{1}{8}(1+g^1)\,(1-g^2)\,(1+g^3)\,(2-g^1+g^2-g^3)$$
$$N^7=-\frac{1}{8}(1+g^1)\,(1+g^2)\,(1+g^3)\,(2-g^1-g^2-g^3)$$
$$N^8=-\frac{1}{8}(1-g^1)\,(1+g^2)\,(1+g^3)\,(2+g^1-g^2-g^3)$$

$$N^9=\frac{1}{4}(1-g^1)\,(1+g^1)\,(1-g^2)\,(1-g^3) \qquad N^{15}=\frac{1}{4}(1-g^1)\,(1+g^1)\,(1+g^2)\,(1+g^3)$$

$$N^{10}=\frac{1}{4}(1-g^2)\,(1+g^2)\,(1+g^1)\,(1-g^3) \qquad N^{16}=\frac{1}{4}(1-g^2)\,(1+g^2)\,(1-g^1)\,(1+g^3)$$

$$N^{11}=\frac{1}{4}(1-g^1)\,(1+g^1)\,(1+g^2)\,(1-g^3) \qquad N^{17}=\frac{1}{4}(1-g^3)\,(1+g^3)\,(1-g^1)\,(1-g^2)$$

$$N^{12}=\frac{1}{4}(1-g^2)\,(1+g^2)\,(1-g^1)\,(1-g^3) \qquad N^{18}=\frac{1}{4}(1-g^3)\,(1+g^3)\,(1+g^1)\,(1-g^2)$$

$$N^{13}=\frac{1}{4}(1-g^1)\,(1+g^1)\,(1-g^2)\,(1+g^3) \qquad N^{19}=\frac{1}{4}(1-g^3)\,(1+g^3)\,(1+g^1)\,(1+g^2)$$

$$N^{14}=\frac{1}{4}(1-g^2)\,(1+g^2)\,(1+g^1)\,(1+g^3) \qquad N^{20}=\frac{1}{4}(1-g^3)\,(1+g^3)\,(1-g^1)\,(1+g^2)$$

Displacements within the volume portion are given by

$$u^i = N^\alpha U_\alpha^i, \tag{2}$$

where the U_α^i represents displacement components of the corner points. The strain-displacement relations are thus

$$\varepsilon_j^i = \frac{1}{2}\left(\frac{\partial u^i}{\partial x^j} + \frac{\partial u^j}{\partial x^i}\right) = \frac{1}{2}\frac{\partial N^\alpha}{\partial g^m}\left(\frac{\partial g^m}{\partial x^j} U_\alpha^i + \frac{\partial g^m}{\partial x^i} U_\alpha^j\right). \tag{3}$$

The strain energy contributed by the material block is thus expressed as

$$E_{(M)} = \frac{1}{2}\left[C_{ik}^{jl}\right]_{(M)}\left[\int \frac{\partial N^\alpha}{\partial g^m}\frac{\partial N^\beta}{\partial g^n}\frac{\partial g^m}{\partial x^j}\frac{\partial g^n}{\partial x^l}\,dv\right]_{(M)} U_\alpha^i\, U_\beta^k, \tag{4}$$

the integration being performed over the volume portion of the material block (M) contained within the element. This defines the stiffness of the material block portion as

$$\left[K_{ik}^{\alpha\beta}\right]_{(M)} = \left[C_{ik}^{jl}\right]_{(M)}\left[\int \frac{\partial N^\alpha}{\partial g^m}\frac{\partial N^\beta}{\partial g^n}\frac{\partial g^m}{\partial x^j}\frac{\partial g^n}{\partial x^l}\,dv\right]_{(M)}, \tag{5}$$

so that the strain energy can be written as

$$E_{(M)} = \frac{1}{2}\left[K_{ik}^{\alpha\beta}\right]_{(M)} U_{\alpha}^{i}\, U_{\beta}^{k}. \tag{6}$$

The components of force contributed by the material block at corner point α are obtained from

$$\frac{\partial E_{(M)}}{\partial U_{\alpha}^{i}} = \left[F_{i}^{\alpha}\right]_{(M)} = \left[K_{ik}^{\alpha\beta}\right]_{(M)} U_{\beta}^{k}. \tag{7}$$

Summing over all material blocks that are common to corner point α, results in an expression for the net external applied force on that point

$$F_{i}^{\alpha} = \sum_{M}\left[K_{ik}^{\alpha\beta}\right]_{(M)} U_{\beta}^{k}. \tag{8}$$

Assuming a total of Γ corner points contained within the volume of the element, there will be $3 \times \Gamma$ equations of the form (8). Let the first Ω of these corner points correspond to the nodes of the element ($\Omega \leq \Gamma$), the next Δ correspond to corner points lying on the surface of the element at locations other than the element nodes ($0 \leq \Delta \leq (\Gamma-\Omega)$), and the last ($\Gamma-\Omega-\Delta$) correspond to points falling within the interior of the element boundary.

If we represent the material stiffness of the overall element as an equivalent homogeneous anisotropic material with stiffness tensor $\bar{C}_{ik}^{jl}$, then the total strain energy for the element is given by

$$\bar{E} = \frac{1}{2}\,\bar{C}_{ik}^{jl}\left[\int_{\bar{V}} \frac{\partial S^{\gamma}}{\partial q^{m}}\,\frac{\partial S^{\rho}}{\partial q^{n}}\,\frac{\partial q^{m}}{\partial x^{j}}\,\frac{\partial q^{n}}{\partial x^{l}}\,dv\right] U_{\gamma}^{i}\, U_{\rho}^{k}, \tag{9}$$

where $\gamma,\rho=1,...\Omega$ and the integration is over the entire volume of the element, $\bar{V}$; S^γ represents the element deformation shape functions; and q^m are the isoparametric coordinates of the transformation

$$x^i = S^\gamma X_\gamma^i \qquad S^\gamma = S^\gamma(q^1, q^2, q^3), \tag{10}$$

with X_γ^i corresponding to the global coordinates of the node point γ. The force applied to node γ is given by

$$F_i^\gamma = \frac{\partial \bar{E}}{\partial u_\gamma^i} = \bar{C}_{ik}^{jl} \left[\int_{\bar{V}} \frac{\partial S^\gamma}{\partial q^m} \frac{\partial S^\rho}{\partial q^n} \frac{\partial q^m}{\partial x^j} \frac{\partial q^n}{\partial x^l} \, dv \right] U_\rho^k, \tag{11}$$

where $\gamma,\rho=1,...,\Omega$.

To establish the equivalent material stiffness, we equate the expression for total strain energy in the element (9) to the sum of the strain energies contributed by the individual material blocks (6), i.e.,

$$\bar{C}_{ik}^{jl} \left[\int \frac{\partial S^\gamma}{\partial q^m} \frac{\partial S^\rho}{\partial q^n} \frac{\partial q^m}{\partial x^j} \frac{\partial q^n}{\partial x^l} \, dv \right] U_\gamma^i \, U_\rho^k =$$

$$\sum_M \left\{ [K_{ik}^{\gamma\rho}]_{(M)} \, U_\gamma^i \, U_\rho^k + 2 \, [K_{ik}^{\gamma\beta}]_{(M)} \, U_\gamma^i \, U_\beta^k + [K_{ik}^{\beta\omega}]_{(M)} \, U_\beta^i \, U_\omega^k \right\}, \tag{12}$$

where $\gamma,\rho=1,...,\Omega$ and $\beta,\omega=(\Omega+1),...,\Gamma$. For convenience, we define the following:

$$A_{jl}^{\gamma\rho} = \int \frac{\partial S^\gamma}{\partial q^m} \frac{\partial S^\rho}{\partial q^n} \frac{\partial q^m}{\partial x^j} \frac{\partial q^n}{\partial x^l} \, dv \tag{13a}$$

$$B_{ik}^{\gamma\rho} = \sum_M \left[K_{ik}^{\gamma\rho} \right]_{(M)}. \tag{13b}$$

Using this notation, we can write (12) as

$$\bar{C}_{ik}^{jl}\, A_{jl}^{\gamma\rho}\, U_{\gamma}^{i}\, U_{\rho}^{k} = B_{ik}^{\gamma\rho}\, U_{\gamma}^{i}\, U_{\rho}^{k} + 2\, B_{ik}^{\gamma\beta}\, U_{\gamma}^{i}\, U_{\beta}^{k} + B_{ik}^{\beta\omega}\, U_{\beta}^{i}\, U_{\omega}^{k}, \tag{14}$$

where $\gamma,\rho=1,...,\Omega$ and $\beta,\omega=(\Omega+1),...,\Gamma$.

As will be shown, the displacements of corner points $\beta=(\Omega+1),...,\Gamma$ can be expressed as functions of the element node displacements, i.e.,

$$U_{\beta}^{k} = Q_{\beta l}^{k\gamma}\, U_{\gamma}^{l}, \tag{15}$$

where $\gamma=1...\Omega$ and $\beta=(\Omega+1),...,\Gamma$.

Substitution of (15) into (14) thus results in the expression

$$\bar{C}_{ik}^{jl}\, A_{jl}^{\gamma\rho}\, U_{\gamma}^{i}\, U_{\rho}^{k} = B_{ik}^{\gamma\rho}\, U_{\gamma}^{i}\, U_{\rho}^{k} + 2\, B_{il}^{\gamma\beta}\, Q_{\beta k}^{l\rho}\, U_{\gamma}^{i}\, U_{\rho}^{k}\frac{\overline{a}}{c}\overline{b} + B_{jl}^{\beta\omega}\, Q_{\beta i}^{j\gamma}\, Q_{\omega k}^{l\rho}\, U_{\gamma}^{i}\, U_{\rho}^{k}, \tag{16}$$

where $\gamma,\rho=1,...,\Omega$ and $\beta,\omega=(\Omega+1),...,\Gamma$.

If we now take the derivative of (16) with respect to the displacement of an arbitrary element node α in degree-of-freedom m, we obtain $3 \times \Omega$ equations:

$$\bar{C}_{mk}^{jl}\, A_{jl}^{\alpha\rho}\, U_{\rho}^{k} = \left[\, B_{mk}^{\alpha\rho} + B_{ml}^{\alpha\beta}\, Q_{\beta k}^{l\rho} + B_{kl}^{\rho\beta}\, Q_{\beta m}^{l\alpha} + B_{jl}^{\beta\omega}\, Q_{\beta m}^{j\alpha}\, Q_{\omega k}^{l\rho} \,\right] U_{\rho}^{k}, \tag{17}$$

where $\alpha,\rho=1,...,\Omega$ and $\beta,\omega=(\Omega+1),...,\Gamma$.

Since the $U_\rho^{\ k}$ are independent of each other, we obtain the relations

$$\bar{C}_{ik}^{\ jl}\, A_{jl}^{\gamma\rho} = B_{ik}^{\gamma\rho} + B_{im}^{\gamma\beta}\, Q_{\beta k}^{m\rho} + B_{km}^{\rho\beta}\, Q_{\beta i}^{m\gamma} + B_{lm}^{\beta\omega}\, Q_{\beta i}^{l\gamma}\, Q_{\omega k}^{m\rho}, \tag{18}$$

where $\gamma,\rho=1,...,\Omega$ and $\beta,\omega=(\Omega+1),...,\Gamma$.

Recalling that from the transformation (10) we have,

$$\frac{\partial x^{\,i}}{\partial q^{\,m}} = \frac{\partial S^{\,\gamma}}{\partial q^{\,m}}\, X_\gamma^{\ i}, \tag{19}$$

and using the relations

$$\frac{\partial x^{\,i}}{\partial q^{\,m}}\,\frac{\partial q^{\,m}}{\partial x^{\,j}} = \frac{\partial S^{\,\gamma}}{\partial q^{\,m}}\,\frac{\partial q^{\,m}}{\partial x^{\,j}}\, X_\gamma^{\ i} = \delta_j^i,$$

which are a consequence of the chain rule for partial differentiation, we can multiply expression (13a) by $X_\gamma^{\ i}\, X_\rho^{\ k}$ to obtain

$$A_{jl}^{\gamma\rho}\, X_\gamma^{\ i}\, X_\rho^{\ k} = \int_{\bar{V}} \frac{\partial S^{\,\gamma}}{\partial q^{\,m}}\,\frac{\partial S^{\,\rho}}{\partial q^{\,n}}\,\frac{\partial q^{\,m}}{\partial X^{\,j}}\,\frac{\partial q^{\,n}}{\partial X^{\,l}}\, X_\gamma^{\ i}\, X_\rho^{\ k}\, dv = \bar{V}\,\delta_j^i\,\delta_l^k, \tag{20}$$

where $\bar{V}$ is the total volume of the element, and δ_j^i is the Kronecker delta.

Multiplying expression (18) by $X_\gamma^{\ r}\, X_\rho^{\ s}$ thus results in

$$\bar{C}_{ik}^{\ jl}\, A_{jl}^{\gamma\rho}\, X_\gamma^{\ r}\, X_\rho^{\ s} = \bar{C}_{ik}^{\ rs}\,\bar{V} = \left[B_{ik}^{\gamma\rho} + B_{im}^{\gamma\beta}\, Q_{\beta k}^{m\rho} + B_{km}^{\rho\beta}\, Q_{\beta i}^{m\gamma} + B_{lm}^{\beta\omega}\, Q_{\beta i}^{l\gamma}\, Q_{\omega k}^{m\rho}\right] X_\gamma^{\ r}\, X_\rho^{\ s}, \tag{21}$$

where $\gamma,\rho=1,...,\Omega$ and $\beta=(\Omega+1),...,\Gamma$, or, upon dividing by the element volume, we arrive at an expression for the equivalent element material stiffness tensor; i.e.,

$$\bar{C}_{ik}^{jl} = \frac{1}{\bar{V}} \left[B_{ik}^{\gamma\rho} + B_{im}^{\gamma\beta} Q_{\beta k}^{m\rho} + B_{km}^{\rho\beta} Q_{\beta i}^{m\gamma} + B_{mn}^{\beta\omega} Q_{\beta i}^{m\gamma} Q_{\omega k}^{n\rho} \right] X_{\gamma}^{j} X_{\rho}^{l}, \tag{22}$$

where $\gamma,\rho=1,...,\Omega$ and $\beta=(\Omega+1),...,\Gamma$.

It remains to develop the coefficients $Q_{\beta l}^{k\gamma}$ in equation (15), which expresses the displacements of the corner points $(\Omega+1)$ through Γ in terms of the displacements of the element nodes.

For the Δ corner points lying on the surface of the element, we require that the net force on these points in any direction tangent to the surface be set to zero, and also that the point remains on the surface as the element deforms. The transformation relations between global cartesian coordinates (x^1, x^2, x^3) and isoparametric coordinates (q^1, q^2, q^3) must be developed to incorporate these constraints.

At the location of one of the corner points ν $((\Omega+1) \le \nu \le (\Omega+\Delta))$, an arbitrary differential length vector can be expressed in the global cartesian frame as

$$d\vec{s} = dx^{i} \hat{I}_{i}, \tag{23}$$

where $\hat{I}_1$, $\hat{I}_2$, $\hat{I}_3$ correspond to the units vectors along the global cartesian coordinate directions. From the transformation (10) we obtain

$$dx^{i} = \frac{\partial x^{i}}{\partial q^{k}} dq^{k}, \tag{24}$$

so that

$$d\vec{s} = \frac{\partial x^{i}}{\partial q^{k}} dq^{k} \hat{I}_{i}. \tag{25}$$

We define the basis vectors for the isoparametric coordinates as

$$\vec{b}_k = \frac{\partial x^i}{\partial q^k} \hat{I}_i, \tag{26}$$

to obtain

$$d\vec{s} = \vec{b}_k dq^k, \tag{27}$$

in the isoparametric system. From this we obtain the second rank metric tensor,

$$g_{kl} = \vec{b}_k \cdot \vec{b}_l = \frac{\partial x^i}{\partial q^k} \frac{\partial x^i}{\partial q^l}. \tag{28}$$

In general, the basis vectors of the isoparametric system are not orthogonal so that the off-diagonal components of the metric tensor are not zero. The basis vectors are tangent to the isoparametric coordinate curves at the point v. Since the element surface on which v lies corresponds to a surface where one of the coordinates, say q^k, is a constant, the basis vectors, tangent to the other two coordinate curves at v, are tangent to the element surface at v, (i.e., $\left(\vec{b}_m\right)^{(k)}$ and $\left(\vec{b}_n\right)^{(k)}$ ($m \neq k$ and $n \neq k$) lie along tangents to the element surface at v, with the surface corresponding to q^k = constant in the isoparametric system).

From (28) we can develop unit tangent vectors along the surface, given by

$$\left(\hat{e}_m\right)^{(k)}_{(v)} = \frac{1}{\sqrt{\underline{g_{mm}}}} \left(\vec{b}_m\right)^{(k)}_{(v)} \text{ and } \left(\hat{e}_n\right)^{(k)}_{(v)} = \frac{1}{\sqrt{\underline{g_{nn}}}} \left(\vec{b}_n\right)^{(k)}_{(v)}, \tag{29}$$

where the line under the repeated indices indicates that summation has been suspended.

We can develop the reciprocal base vectors for the isoparametric system from the vector cross products

$$\vec{b}^1 = \frac{1}{\sqrt{g}}\,\vec{b}_2 \times \vec{b}_3,\quad \vec{b}^2 = \frac{1}{\sqrt{g}}\,\vec{b}_3 \times \vec{b}_1,\quad \vec{b}^3 = \frac{1}{\sqrt{g}}\,\vec{b}_1 \times \vec{b}_2, \tag{30}$$

where $g = \det g_{kl}$. (31)

These relations can be written more compactly as

$$\vec{b}^k = \frac{1}{2\sqrt{g}}\varepsilon^{kmn}\left(\vec{b}_m\right)^{(k)} \times \left(\vec{b}_n\right)^{(k)}, \tag{32}$$

where ε^{kmn} is the familiar permutation symbol, i.e.,

$\varepsilon^{kmn} = 1$ if k, m, n is an even permutation of 1, 2, 3;
$\varepsilon^{kmn} = -1$ if k, m, n is an odd permuatation of 1, 2, 3; and
$\varepsilon^{kmn} = 0$ if any two indices are the same.

The reciprocal base vector $\left[\vec{b}^{\,k}\right]_{(v)}$ at v is therefore in the direction normal to the element surface corresponding to q^k = constant, i.e.,

if the surface corresponds to q^1 = constant, $\left[\vec{b}^{\,1}\right]_{(v)}$ lies along the normal and $\left[\hat{e}_2\right]_{(v)}$ and $\left[\hat{e}_3\right]_{(v)}$ are tangents to the surface;

if the surface corresponds to q^2 = constant, $\left[\vec{b}^{\,2}\right]_{(v)}$ lies along the normal and $\left[\hat{e}_3\right]_{(v)}$ and $\left[\hat{e}_1\right]_{(v)}$ are tangents to the surface; and

if the surface corresponds to q^3 = constant, $\left[\vec{b}^{\,3}\right]_{(v)}$ lies along the normal and $\left[\hat{e}_1\right]_{(v)}$ and $\left[\hat{e}_2\right]_{(v)}$ are tangents to the surface.

We now define the contravarient second rank tensor

$$g^{kl} = \vec{b}^{k} \cdot \vec{b}^{l}. \tag{33}$$

This now allows us to express the unit normal at the point v as

$$\left(\hat{e}^{k}\right)_{(v)} = \frac{1}{\sqrt{g^{\underline{kk}}}} \left(\vec{b}^{k}\right)_{(v)}. \tag{34}$$

The definitions (29) and (34) allow us to apply the necessary constraints for the corner points (Ω+1) through (Ω+Δ). The surface corner points must first, however, be categorized according to whether a point lies along one of the edges of the element, or whether it lies on an element face. Let the points (Ω+1) through (Ω+E), $0 \le E \le \Delta$, correspond to the surface corner points lying on the edge of the element, and the points (Ω+E+1) through (Ω+Δ) correspond to the remaining corner points that lie on the element faces.

For surface corner points lying along an element edge assume that the corner point v lies on an element edge corresponding to the coordinate curve q^{r}. From expression (32), the reciprocal base vectors at point v are defined as

$$(\vec{b}^{k})_{(v)} = \frac{1}{2\sqrt{g}} \varepsilon^{kmn} (\vec{b}_{m})_{(v)} \times (\vec{b}_{n})_{(v)}. \tag{35}$$

We require the displacement components at v to be constrained along the direction of $\vec{b}^{k}(k \neq r)$ such that the point remains on the surface q^{k} = constant, corresponding to each of the two element faces that intersect at the edge. The constraint is thus expressed as

$$U_{v}^{i} \hat{I}_{i} \cdot (\hat{e}^{k})_{\underline{(v)}} = S^{\rho}(q^{1}, q^{2}, q^{3})_{(v)} U_{\rho}^{i} \hat{I}_{i} \cdot (\hat{e}^{k})_{\underline{(v)}}, \tag{36}$$

where $\rho=1,...,\Omega$ and $\nu=(\Omega+1),...,(\Omega+E)$, with $(\hat{e}^{\,k})_{(\nu)}$ representing the unit vector along the direction of $(\vec{b}^{\,k})_{(\nu)}$ as defined in (34).

Since $\vec{b}_m = \dfrac{\partial x^{\,i}}{\partial q^{\,m}} \hat{I}_i$, we can write

$$\vec{b}^{\,k} = \frac{1}{2\sqrt{g}} \varepsilon^{kmn} \frac{\partial x^{\,i}}{\partial q^{\,m}} \frac{\partial x^{\,j}}{\partial q^{\,n}} \hat{I}_i \times \hat{I}_j \tag{37}$$

or

$$\vec{b}^{\,k} = \frac{1}{2\sqrt{g}} \varepsilon^{kmn} \varepsilon_{ijl} \frac{\partial x^{\,i}}{\partial q^{\,m}} \frac{\partial x^{\,j}}{\partial q^{\,n}} \hat{I}_l, \tag{38}$$

where we have used the expression for the vector cross product

$$\hat{I}_i \times \hat{I}_j = \varepsilon_{ijl} \hat{I}_l. \tag{39}$$

The displacement constraints at point ν lying on an element edge corresponding to the isoparametric coordinate curve q^r can thus be written as

$$\frac{1}{2\sqrt{g}\sqrt{g^{\underline{kk}}}} \varepsilon^{kmn} \varepsilon_{ijl} \frac{\partial x^{\,i}}{\partial q^{\,m}} \frac{\partial x^{\,j}}{\partial q^{\,n}} U_\nu^{\,l} = \frac{1}{2\sqrt{g}\sqrt{g^{\underline{kk}}}} \varepsilon^{kmn} \varepsilon_{ijl} \frac{\partial x^{\,i}}{\partial q^{\,m}} \frac{\partial x^{\,i}}{\partial q^{\,n}} S^{\rho}(q^1,q^2,q^3)_{(\nu)} U_\rho^{\,l}, \tag{40}$$

or

$$\varepsilon^{kmn} \varepsilon_{ijl} \frac{\partial x^{\,i}}{\partial q^{\,m}} \frac{\partial x^{\,j}}{\partial q^{\,n}} U_\nu^{\,l} = \varepsilon^{kmn} \varepsilon_{ijl} \frac{\partial x^{\,i}}{\partial q^{\,m}} \frac{\partial x^{\,j}}{\partial q^{\,n}} S^{\rho}(q^1,q^2,q^3)_{(\nu)} U_\rho^{\,l}, \tag{41}$$

where $k \neq r$, $\rho=1,...,\Omega$, and $\nu=(\Omega+1),...,(\Omega+E)$, and where it is understood that the expression is to be evaluated at the point ν.

The third constraint expression is provided by the requirement for zero force along the coordinate curve q^r at ν. To impose this condition, we first write (8) using the definition (13b), i.e.,

$$F_i^{\nu} = B_{ik}^{\nu\rho} U_{\rho}^{\ k} + B_{ik}^{\nu\omega} U_{\omega}^{\nu}\ B_{ik}^{\nu\mu} U_{\mu}^{\ k} + B_{ik}^{\nu\zeta} U_{\zeta}^{\ k}, \tag{42}$$

where $\rho=1,...,\Omega$, ν, $\omega=(\Omega+1),...,(\Omega+E)$, $\mu=(\Omega+E+1),...,(\Omega+\Delta)$, and $\zeta=(\Omega+\Delta+1),...,\Gamma$.

From (26), the basis vector tangent to the coordinate curve q^r is expressed as

$$\vec{b}_r = \frac{\partial x^{\ i}}{\partial q^{\ r}} \hat{I}_i. \tag{43}$$

The condition for zero force along q^r can thus be enforced by forming the vector dot product of (42) with (43) and setting the result to zero, i.e.,

$$F_i^{\nu} \hat{I}_i \cdot \left(\vec{b}_r\right)_{(\underline{\nu})} = 0, \tag{44}$$

or,

$$\frac{\partial x^{\ i}}{\partial q^{\ r}} B_{il}^{\nu\omega} U_{\omega}^{\ l} + \frac{\partial x^{\ i}}{\partial q^{\ r}} B_{il}^{\nu\mu} U_{\mu}^{\ l} + \frac{\partial x^{\ i}}{\partial q^{\ r}} B_{il}^{\nu\zeta} U_{\zeta}^{\ l} = - \frac{\partial x^{\ i}}{\partial q^{\ r}} B_{il}^{\nu\rho} U_{\rho}^{\ l}, \tag{45}$$

r corresponds to coordinate curve q^r along the element edge where $\rho=1,...,\Omega$, $\nu,\omega=(\Omega+1),...,(\Omega+E)$, $\mu=(\Omega+E+1),...,(\Omega+\Delta)$, and $\zeta=(\Omega+\Delta+1),...,\Gamma$.

For surface corner points lying on an element face, in the case where point ν represents a corner point lying on the element face corresponding to q^k = constant, expression (41) provides only one constraint equation, restricting the displacement components of point ν such that it remains on the surface whose normal is $(\hat{e}^{\ k})_{(\nu)}$ i.e.,

$$\varepsilon^{kmn}\,\varepsilon_{ijl}\,\frac{\partial x^{\,i}}{\partial q^{\,m}}\,\frac{\partial x^{\,j}}{\partial q^{\,n}}\,U_{\nu}^{\,l} = \varepsilon^{kmn}\,\varepsilon_{ijl}\,\frac{\partial x^{\,i}}{\partial q^{\,m}}\,\frac{\partial x^{\,j}}{\partial q^{\,n}}\,S^{\rho}(q^{\,1},q^{\,2},q^{\,3})_{(\nu)}\,U_{\rho}^{\,l}, \tag{46}$$

where k corresponds to q^k = constant, $\rho=1,\ldots,\Omega$, and $\nu=(\Omega+E+1),\ldots,(\Omega+\Delta)$.

The other two constraint equations are obtained from the requirement for zero force along the directions tangent to the element face at point ν, i.e.,

$$F_i^{\nu}\hat{I}_i \cdot \left[\hat{e}_m\right]_{(\underline{\nu})}^{(k)} = 0, \text{ and } F_i^{\nu}\hat{I}_i \cdot \left[\hat{e}_n\right]_{(\underline{\nu})}^{(k)} = 0, \tag{47}$$

with $\left[\hat{e}_m\right]_{(\nu)}^{(k)}$ and $\left[\hat{e}_n\right]_{(\nu)}^{(k)}$ defined in (29) and corresponding to unit surface tangent vectors at point ν on the element surface representing q^k = constant.

These conditions lead to two equations of the form (45),

$$\frac{\partial x^{\,i}}{\partial q^{\,r}}\,B_{il}^{\nu\omega}\,U_{\omega}^{\,l} + \frac{\partial x^{\,i}}{\partial q^{\,r}}\,B_{il}^{\nu\mu}\,U_{\mu}^{\,l} + \frac{\partial x^{\,i}}{\partial q^{\,r}}\,B_{il}^{\nu\zeta}\,U_{\zeta}^{\,l} = -\,\frac{\partial x^{\,i}}{\partial q^{\,r}}\,B_{il}^{\nu\rho}\,U_{\rho}^{\,l}, \tag{48}$$

where $r\neq k$, $\rho=1,\ldots,\Omega$, $\omega=(\Omega+1),\ldots,(\Omega+E)$, $\nu,\mu=(\Omega+E+1),\ldots,(\Omega+\Delta)$, $\zeta=(\Omega+\Delta+1),\ldots,\Gamma$, and where it is again understood that (46) and (48) are to be evaluated at the point ν.

For the remaining corner points ($(\Omega+\Delta+1)$ through Γ) that lie internally within the element's boundaries, we require zero net force in all directions. Expression (42), with the left-hand side set to zero, provides the constraint equations for these internal points, resulting in

$$B_{ik}^{\nu\omega}U_{\omega}^{\,k} + B_{ik}^{\nu\xi}U_{\mu}^{\,k} + B_{ik}^{\nu\xi}U_{\xi}^{\,k} = -\,B_{ik}^{\nu\rho}U_{\rho}^{\,k}, \tag{49}$$

where $i=1,2,3$, $(\rho=1,\ldots,\Omega)$, $(\omega=(\Omega+1),\ldots,(\Omega+E))$, $(\mu=(\Omega+E+1),\ldots,(\Omega+\Delta))$, and $(\nu,\xi=(\Omega+\Delta+1),\ldots,\Gamma)$.

Expressions (41), (45), (46), (48), and (49) together form a system of $3x(\Gamma-\Omega)$ equations in the $3x(\Gamma-\Omega)$ unknown displacements for the Δ surface corner points and the $(\Gamma-\Omega-\Delta)$ internal corner points. This system of equations can be solved to obtain the relations (15), expressing the displacement components of all non-nodel corner points in terms of the displacement components of the elements nodes.

Wedge Prismatic Elements

The constraint equations developed above are suitable for rectangular prismatic elements where the edges align with the isoparametric coordinate curves. For wedge prismatic elements, an alternate set of constraint equations must be employed for corner points lying on the element surface.

We shall assume that the isoparametric representation of the wedge prismatic element is such that the two triangular faces correspond to surfaces of q^3 = constant, and that two adjacent four-noded faces of the element correspond with the surfaces $q^1 = 0$ and $q^2 = 0$, in a manner that forms a right-handed frame of reference. The intersection of the third four-noded face with a surface represented by q^3 = constant results in a curve represented by $q^2 = 1 - q^1$. A vector lying tangent to this curve at a point v can be written in terms of the basis vectors as

$$(\vec{C})_{(v)} = (\vec{b}_1)_{(v)} - (\vec{b}_2)_{(v)} = \left(\frac{\partial x^i}{\partial q^1} - \frac{\partial x^i}{\partial q^2}\right)_{(v)} \hat{I}_i, \tag{50}$$

$(\vec{C})_{(r)}$ and the basis vector $(\vec{b}_3)_{(v)}$ thus represent two independent vectors that are tangent to the third four-noded element face at the point v.

The normal to this element face at point v can be obtained from the cross product

$$\vec{N}_{(v)} = (\vec{C})_{(v)} \times (\vec{b}_3)_{(v)} = \left(\frac{\partial x^i}{\partial q^1} - \frac{\partial x^i}{\partial q^2}\right)_{(v)} \hat{I}_i \times \left(\frac{\partial x^j}{\partial q^3}\right)_{(v)} \hat{I}_j, \tag{51}$$

or

$$\vec{N}_{(v)} = \varepsilon_{ijk} \left(\frac{\partial x^i}{\partial q^1} - \frac{\partial x^i}{\partial q^2} \right)_v \left(\frac{\partial x^j}{\partial q^3} \right)_v \hat{I}_k. \tag{52}$$

The constraint equations for wedge prismatic elements can now be developed. As with the rectangular prismatic elements, we must distinguish between surface corner points that lie on an element edge (i.e., points (Ω+1) through (Ω+E)), and surface corner points that lie on element faces ((Ω+E+1) through (Ω+Δ)).

For surface corner points lying along an element edge, the two displacement constraint equations provided by (41), and the force constraint equation provided by (45) are applicable to those surface corner points lying on wedge prismatic element edges that are aligned with the q^1, q^2, and q^3 coordinate curves. The only two element edges for which the constraint equations (41) and (45) do not apply, are the edges corresponding to $q^2 = 1 - q^1$ on the two triangular faces of the element.

Since the triangular faces correspond to surfaces q^3 = constant, the normal to these faces at a point ν is obtained from the reciprocal base vector given by (38), i.e.,

$$(\vec{b}^3)_{(v)} = \frac{1}{2\sqrt{g}} \varepsilon^{3mn} \varepsilon_{ijk} \left(\frac{\partial x^i}{\partial q^m} \frac{\partial x^i}{\partial q^n} \right)_{(v)} \hat{I}_k. \tag{53}$$

The constraint equations for a point ν lying on one of the edges corresponding to $q^2 = 1 - q^1$ are thus obtained as follows along the direction $\vec{N}_{(v)}$, we enforce the displacement constraint

$$\vec{N}_{\underline{(v)}} \cdot U_{\underline{v}}^{\ 1} \hat{I}_1 = \vec{N}_{\underline{v}} \cdot S^{\rho}(q^1, q^2, q^3)_{\underline{(v)}} \ U_{\rho}^{\ 1} \hat{I}_1, \tag{54}$$

where $\rho=1,...,\Omega$ and $\nu=(\Omega+1),...,(\Omega+E)$, so that,

$$\varepsilon_{ijl}\left(\frac{\partial x^i}{\partial q^1}-\frac{\partial x^i}{\partial q^2}\right)_{(\underline{\nu})}\left(\frac{\partial x^j}{\partial q^3}\right)_{(\underline{\nu})} U_{\underline{\nu}}^{l}=\varepsilon_{ijl}\left(\frac{\partial x^i}{\partial q^1}-\frac{\partial x^i}{\partial q^2}\right)_{(\underline{\nu})}\left(\frac{\partial x^j}{\partial q^3}\right)_{(\underline{\nu})} S^{\rho}(q^1,q^2,q^3)_{(\underline{\nu})}\, U_{\rho}^{l}, \quad (55)$$

where $\rho=1,...,\Omega$ and $\nu=(\Omega+1),...,(\Omega+E)$.

Along the direction $(\vec{b}^3)_{(\nu)}$, the required displacement constraint is

$$(\vec{b}^3)_{(\underline{\nu})}\cdot U_{\underline{\nu}}^{l}\,\hat{I}_l=(\vec{b}^3)_{\nu}\cdot S^{\rho}(q^1,q^2,q^3)_{(\nu)}\, U_{\rho}^{l}\,\hat{I}_l, \quad (56)$$

where $\rho=1,...,\Omega$ and $\nu=(\Omega+1),...,(\Omega+E)$; or,

$$\varepsilon^{3mn}\,\varepsilon_{ijl}\left(\frac{\partial x^i}{\partial q^m}-\frac{\partial x^j}{\partial q^n}\right)_{(\underline{\nu})} U_{\underline{\nu}}^{l}=\varepsilon^{3mn}\,\varepsilon_{ijl}\left(\frac{\partial x^i}{\partial q^m}-\frac{\partial x^j}{\partial q^n}\right)_{(\underline{\nu})} S^{\rho}(q^1,q^2,q^3)_{(\underline{\nu})}\, U_{\rho}^{l}, \quad (57)$$

where $\rho=1,...,\Omega$, and $\nu=(\Omega+1),...,(\Omega+E)$, and along the direction $(\vec{C})_{(\nu)}$, which is tangent to the edge at ν, we require the force to be zero, i.e.,

$$(\vec{C})_{(\underline{\nu})}\cdot F_i^{\nu_\rho}\hat{I}_i=0, \quad (58)$$

resulting in

$$\left(\frac{\partial x^i}{\partial q^1}-\frac{\partial x^i}{\partial q^2}\right)_{(\underline{\nu})}\left(B_{il}^{\nu\omega}\,U_{\omega}^{l}+B_{il}^{\nu\mu}\,U_{\mu}^{l}+B_{il}^{\nu\zeta}\,U_{\zeta}^{l}\right)=-\left(\frac{\partial x^i}{\partial q^1}-\frac{\partial x^i}{\partial q^2}\right)_{(\underline{\nu})} B_{il}^{\nu\rho}\,U_{\rho}^{l}, \quad (59)$$

where $\rho=1,...,\Omega$, $\nu,\omega=(\Omega+1),...,(\Omega+E)$, $\mu=(\Omega+E+1),...,(\Omega+\Delta)$, and $\zeta=(\Omega+\Delta+1),...,\Gamma$.

For surface corner points lying on an element face, only those corner points lying on the element face whose normal is given by (52) require constraint equations that are different from (46) and (48).

Expressions (55) and (59) provide two of the constraint equations, except with ν corresponding to points (Ω+E+1) through (Ω+Δ). The third constraint equation corresponds to the requirement for zero force along the direction of the basis vector $(\vec{b}_3)_{(r)}$ that can be obtained from (48) by setting r = 3, i.e.,

$$\frac{\partial x^i}{\partial q^3} B_{il}^{\nu\omega} U_\omega^l + \frac{\partial x^i}{\partial q^3} B_{il}^{\nu\mu} U_\mu^l + \frac{\partial x^i}{\partial q^3} B_{il}^{\nu\zeta} U_\zeta^l = - \frac{\partial x^i}{\partial q^3} B_{il}^{\nu\rho} U_\rho^l, \tag{60}$$

where ρ=1,...,Ω, ω=(Ω+1),...,(Ω+E), ν,μ=(Ω+E+1),...,(Ω+Δ), and ζ=(Ω+Δ+1),...,Γ.

Expressions (55), (57), and (59) for surface corner points lying on the edges corresponding to $q^2=1-q^1$, and (55), (59), and (60) for surface corner points lying on the element face that is not aligned with the isoparametric coordinate surfaces, can be used with wedge prismatic elements to obtain three equations for the unknown displacement components of the surface corner points. These relations, together with the equations provided in (41), (45), (46), (48), and (49) for the other non-nodal corner points, can be grouped to form the 3x(Γ-Ω) equations required for obtaining the relations (15), when wedge prismatic elements are incorporated.

3. RESULTS

In this section, the effective stiffness constants, C_{ik}^{jl}, of a four-layered cubic element with rectangular faces are calculated to demonstrate the capability of this newly developed formulation. Results are compared to those calculated by Chou's model showing a significant difference in transverse shear properties. The effects of stacking sequence of layer construction on the effective properties of the element will also be illustrated and discussed in detail.

Figure 4 illustrates the coordinate system and constitutive relation in a four-layer laminated block (0.2 × 0.2 × 0.2 in). Coordinates 1 and 2 are on the plane of laminate plane. The ply orientation is defined as the angle between fiber direction and coordinate 1. A 0° ply has fibers oriented along coordinate 1. The effective stiffness components are illustrated in a contracted notation (C_{ij}, i and

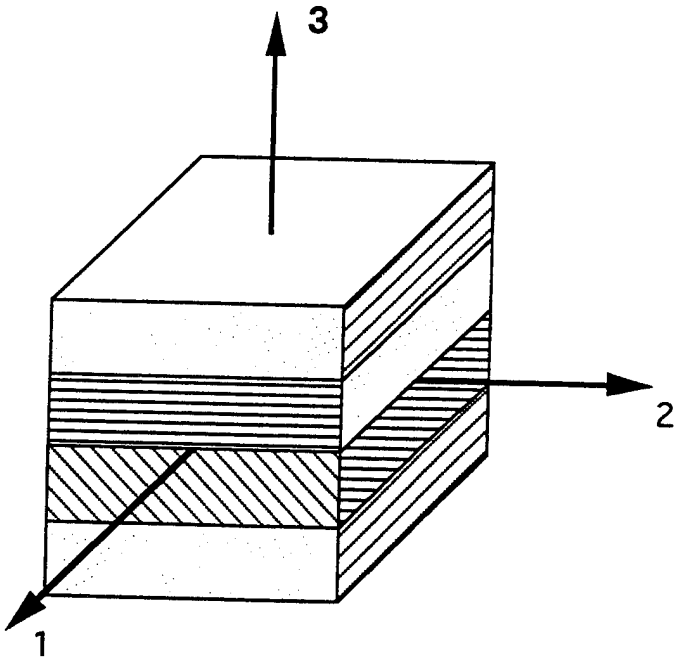

$$\begin{Bmatrix} \sigma_{11} \\ \sigma_{22} \\ \sigma_{33} \\ \tau_{23} \\ \tau_{31} \\ \tau_{12} \end{Bmatrix} = \begin{bmatrix} C_{11} & C_{12} & C_{13} & C_{14} & C_{15} & C_{16} \\ C_{21} & C_{22} & C_{23} & C_{24} & C_{25} & C_{26} \\ C_{31} & C_{32} & C_{33} & C_{34} & C_{35} & C_{36} \\ C_{41} & C_{42} & C_{43} & C_{44} & C_{45} & C_{46} \\ C_{51} & C_{52} & C_{53} & C_{54} & C_{55} & C_{56} \\ C_{61} & C_{62} & C_{63} & C_{64} & C_{65} & C_{66} \end{bmatrix} \begin{Bmatrix} \varepsilon_{11} \\ \varepsilon_{22} \\ \varepsilon_{33} \\ \gamma_{23} \\ \gamma_{31} \\ \gamma_{12} \end{Bmatrix}$$

Figure 4. Constitutive relation for an anisotropic four-layered element.

j = 1 – 6) for convenience. Two layup constructions, a cross-ply [0/0/90/90] and an angle-ply [0/0/45/45], were investigated. Each ply has an equal thickness of 0.05 in. In fact, each ply is composed of 10 unit directional fiber layers with thickness of 0.005 in. The effective properties were calculated based on IM7 graphite/8551 epoxy material whose properties are shown in Table 1. An 8-node element which utilizes linear transform functions in Equation 4 for analysis was used to calculate effective properties of the material block.

Table 1. Material Properties of IM7/8551

E11	=	22.50E6 PSI
E22	=	1.20E6 PSI
E33	=	1.20E6 PSI
v12	=	0.33
v13	=	0.33
v23	=	0.31
G12	=	0.70E6 PSI
G13	=	0.70E6 PSI
G23	=	0.53E6 PSI

3.1 Transverse Shear Properties. Tables 2 and 3 show the comparison of effective stiffness for both layup constructions [0/0/90/90] and 0/0/45/45], respectively. Significant differences on transverse shear properties and shear coupling terms were found for both cases. The transverse shear properties (C_{44} and C_{55}) for a layup construction of [0/0/90/90] are 36% lower than calculated by the new model. The transverse shear properties from Chou's model are basically calculated from a volume average. His model does not account for either continuity or compatibility of the materials through the thickness. A linear deformation was also made by Chou's model. Therefore, the in-plane properties (C_{ij}^{ij}, = 1, 2, and 6) and transverse normal (C_{33}) were found to be identical. These properties are considered to be exact under the assumption.

For an angle-ply layup construction [0/0/45/45], transverse shear properties, C_{44} and C_{55}, are different by 35% and 40%, respectively. The transverse shear coupling terms ($C_{45} = C_{54}$) are 85% of difference. These results further illustrate the importance of the current model. In fact, larger errors may be obtained for an element with more complex ply orientations, stacking sequence, or various ply thicknesses by using the "volume average" approach.

As discussed previously, both "volume average" and "plate theory" approaches cannot accurately calculate effective properties in the transverse direction. For a thick-section structure, the transverse shear properties are even more important since these structures generally carry more shear loads than thin-shelled structures. For finite element applications, accurate transverse shear properties are especially important since the elements are 3-D blocks with arbitrary shapes.

Table 2. Comparison of the Effective Properties of Cross-Ply Laminates

Chou's Model					
0.1211E+08	0.5883E+06	0.5051E+06	0	0	0
0.5883E+06	0.1211E+08	0.5051E+06	0	0	0
0.5051E+06	0.5051E+06	0.1342E+07	0	0	0
0	0	0	0.6033E+06	0	0
0	0	0	0	0.6033E+06	0
0	0	0	0	0	0.7000E+06
3-D Solid Element Model					
0.1211E+08	0.5883E+06	0.5051E+06	0	0	0
0.5883E+06	0.1211E+08	0.5051E+06	0	0	0
0.5051E+06	0.5051E+06	0.1342E+07	0	0	0
0	0	0	0.4413E+06	0	0
0	0	0	0	0.4413E+06	0
0	0	0	0	0	0.7000E+06

Table 3. Comparison of the Effective Properties of Angle-Ply Laminates

Chou's Model					
0.1497E+08	0.3117E+07	0.5444E+06	0	0	0.2694E+07
0.3117E+07	0.4194E+07	0.4658E+06	0	0	0.2692E+07
0.5444E+06	0.4658E+06	0.1342E+07	0	0	0.3933E+05
0	0	0	0.5670E+06	0.4209E+05	0
0	0	0	0.4209E+05	0.6512E+06	0
0.2694E+07	0.2692E+07	0.3933E+05	0	0	0.3231E+07
3-D Solid Element Model					
0.1497E+08	0.3117E+07	0.5444E+06	0	0	0.2694E+07
0.3117E+07	0.4194E+07	0.4658E+06	0	0	0.2692E+07
0.5444E+06	0.4658E+06	0.1342E+07	0	0	0.3933E+05
0	0	0	0.4182E+06	0.2271E+05	0
0	0	0	0.2271E+05	0.4637E+06	0
0.2694E+07	0.2692E+07	0.3933E+05	0	0	0.3231E+07

3.2 Effects of Stacking Sequence. In general, the plate theory assumes constant transverse shear stress distribution through the thickness. Accordingly, the effective transverse shear constants of a laminate calculated from the plate theory approach are independent of the stacking sequence. Recently, Roy and Kim (1989) showed the effects of stacking sequence on transverse shear properties experimentally. Models based on the deformations of a beam and a ring subjected to specific loading conditions were proposed by Roy and Tsai (1992). Their model reported the dependence of transverse shear properties on stacking sequence. However, only two specific geometries (beam and ring) and loading conditions were considered, and cannot be applied to a generalized case.

Tables 4 and 5 illustrate the variations of electric constants in cross-ply [0/90] and angle-ply [0/45] laminates as functions of stacking sequence, respectively. In the cross-ply laminate case, the shear elastic constant, C_{44}, which corresponds to shear stress and strain in the 2-3 direction (i.e., $\tau 23$ and $\gamma 23$) increases as the 90° plies are located away from the laminate's midplane. The 90° plies have fibers oriented along coordinate 2 and provide more shear stiffness in the 2-3 direction. Thus, the maximum shear stiffness, C_{44}, occurs for the stacking sequence of [90/0/0/90]. On the contrary, the shear elastic constant, C_{55}, which corresponding to shear stress and strain in the 1-3 direction ($\tau 13$ and $\gamma 13$) decreases as the 90° plies are moved away from laminate's midplane. Since the 0° layers give a higher shear stiffness in this particular direction, the laminate with layup construction of [90/0/0/90] has the smallest shear constant, C_{55}.

Similar effects of stacking sequence on transverse shear constants, C_{44} and C_{55}, and shear couplings, C_{45} and C_{54}, were observed for laminates with angle-ply [0/45] construction shown in Table 5. The same conclusions can be drawn as those discussed in the previous section for the cross-ply laminates. The shear elastic constant, C_{44}, which corresponds to shear stress and strain in the 2-3 direction (i.e., $\tau 23$ and $\gamma 13$), decreases as the 45° plies are moved away from the laminate's midplane. In general, the effects of stacking sequence are more significant for an element with irregular cross sections, complex layup constructions, and nonsymmetric stacking sequence.

4. FINITE ELEMENT APPLICATIONS

A finite element preprocessor was developed to generate finite element meshes with specific geometries. The effective properties of each element are calculated individually based on the model. Figure 5 shows the finite element model of a composite rocket motor case generated by the preprocessor.

Table 4. Effects of Stacking Sequence on Transverse Shear Properties of Cross-Ply Laminates

[0/90/90/0]					
0.1211E+08	0.5883E+06	0.5051E+06	0	0	0
0.5883E+06	0.1211E+08	0.5051E+06	0	0	0
0.5051E+06	0.5051E+06	0.1342E+07	0	0	0
0	0	0	0.4278E+06	0	0
0	0	0	0	0.4556E+06	0
0	0	0	0	0	0.7000E+06
[0/0/90/90]					
0.1211E+08	0.5883E+06	0.5051E+06	0	0	0
0.5883E+06	0.1211E+08	0.5051E+06	0	0	0
0.5051E+06	0.5051E+06	0.1342E+07	0	0	0
0	0	0	0.4413E+06	0	0
0	0	0	0	0.4413E+06	0
0	0	0	0	0	0.7000E+06
[90/0/0/90]					
0.1211E+08	0.5883E+06	0.5051E+06	0	0	0
0.5883E+06	0.1211E+08	0.5051E+06	0	0	0
0.5051E+06	0.5051E+07	0.1342E+07	0	0	0
0	0	0	0.4556E+06	0	0
0	0	0	0	0.4278E+06	0
0	0	0	0	0	0.7000E+06

Table 5. Effects of Stacking Sequence on Transverse Shear Properties of Angle-Ply Laminates

[0/45/45/0]					
0.1497E+08	0.3117E+07	0.5444E+06	0	0	0.2694E+07
0.3117E+07	0.4194E+07	0.4658E+06	0	0	0.2692E+07
0.5444E+06	0.4658E+06	0.1342E+07	0	0	0.3933E+05
0	0	0	0.4114E+06	0.1576E+05	0
0	0	0	0.3138E+05	0.5925E+06	0
0.2694E+07	0.2692E+07	0.3993E+05	0	0	0.3231E+07
[0/0/45/45]					
0.1497E+08	0.3117E+07	0.5444E+06	0	0	0.2694E+07
0.3117E+07	0.4194E+07	0.4658E+06	0	0	0.2692E+07
0.5444E+06	0.4658E+06	0.1342E+07	0	0	0.3933E+05
0	0	0	0.5167E+06	0.3441E+05	0
0	0	0	0.3441E+05	0.5881E+06	0
0.2694E+07	0.2692E+07	0.3933E+05	0	0	0.3231E+07
[45/0/0/45]					
0.1497E+08	0.3117E+07	0.5444E+06	0	0	0.2694E+07
0.3117E+07	0.4194E+07	0.4658E+06	0	0	0.2692E+07
0.5444E+06	0.4658E+06	0.1342E+07	0	0	0.3933E+05
0	0	0	0.5204E+06	0.3746E+05	0
0	0	0	0.3746E+05	0.5835E+06	0
0.2694E+07	0.2692E+07	0.3933E+05	0	0	0.3231E+07

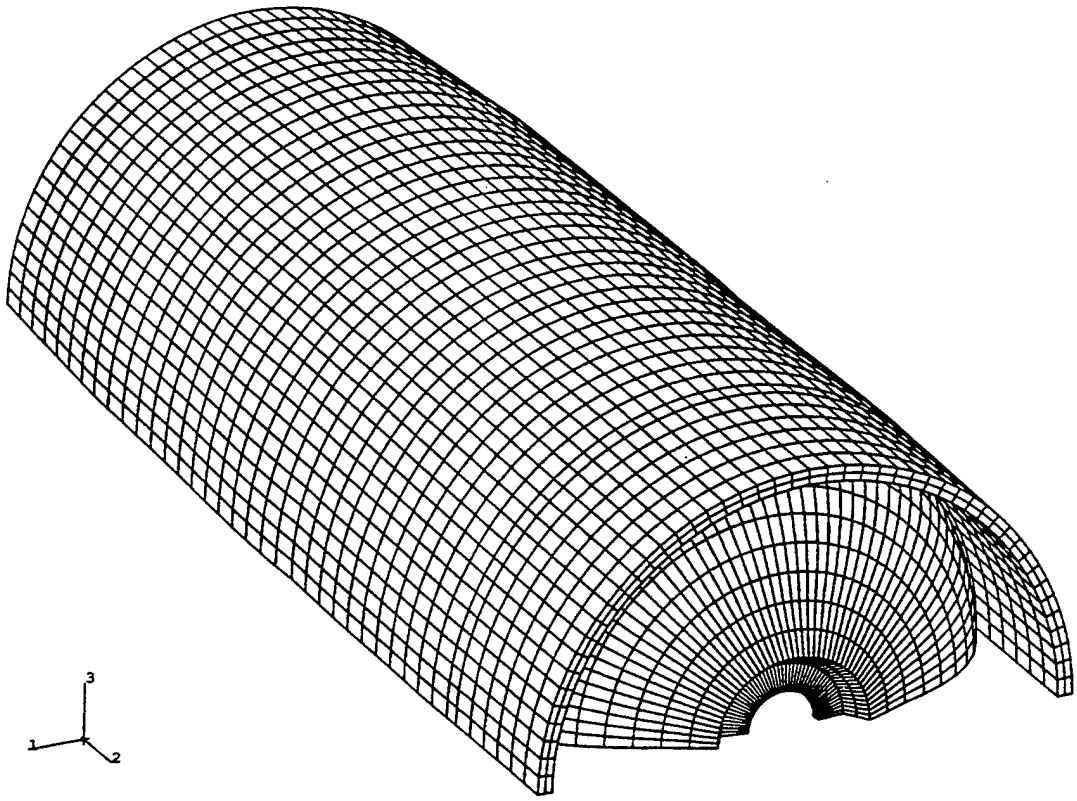

Figure 5. Finite element model for a composite rocket motor case.

The motor case consists of two filament-wound composite components. The case's inner region is a helically wound bottle with a geodesic winding pattern. The outer region of the motor case is a cylinder with a cross-ply layup construction. In addition, both the inner and outer cases were constructed with graphite and glass composites.

The thickness of the composite varies along the axial direction in both the inner and outer cases, as shown in Figure 6. Due to the complexity of case geometry, the general elements are not rectangular and vary along the arc length. The elements are arbitrarily shaped and contain several plies with various fiber orientations and materials through the thickness in some areas. In fact, it is typically a finite element model used in a real-world application; the capability to determine the effective properties in the proposed model is indeed needed.

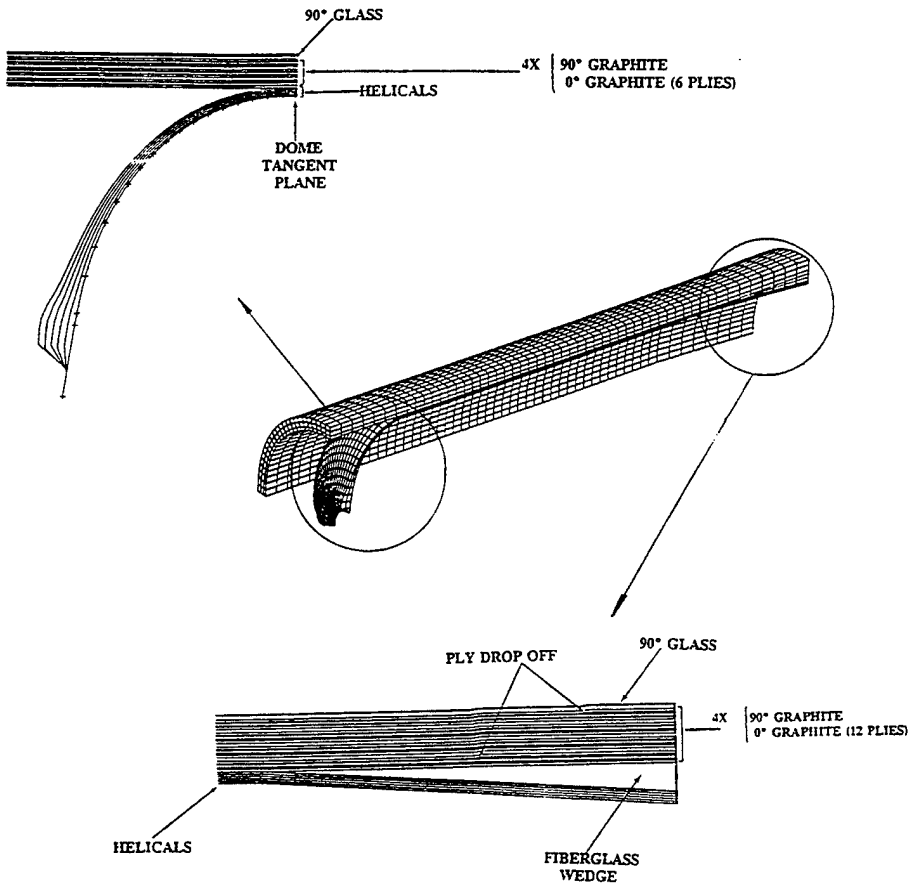

Figure 6. Laminate construction of the composite case.

For a geodesic winding, the fibers are placed along the shortest path on the case surface and the winding angle (i.e., fiber orientation) varies along the path upon the geometry. The winding angles of the innermost layer are illustrated and plotted along the arc length in Figure 7. The winding angles vary dramatically in the dome and nozzle areas. The developed preprocessor calculates the winding angle at each element according to the geodesic path and case geometry. The stiffness components (C^{ij}_{kl},) of the innermost elements along the arc length are illustrated in Figure 8. For the most part, effective properties vary significantly in most materials. The variation is due to the combined effect of various winding angles and layup constructions.

Clearly, the effective properties are essential to achieving an accurate finite element analysis. Currently, all the commercial packages were developed using either "volume average" or "laminated plate theory" to determine the effective properties. In general, the results are poor for structural analyses with complex geometries and layup constructions. In fact, ABAQUS suggests that no skewed elements be used in the finite element model to improve the accuracy of analyses.

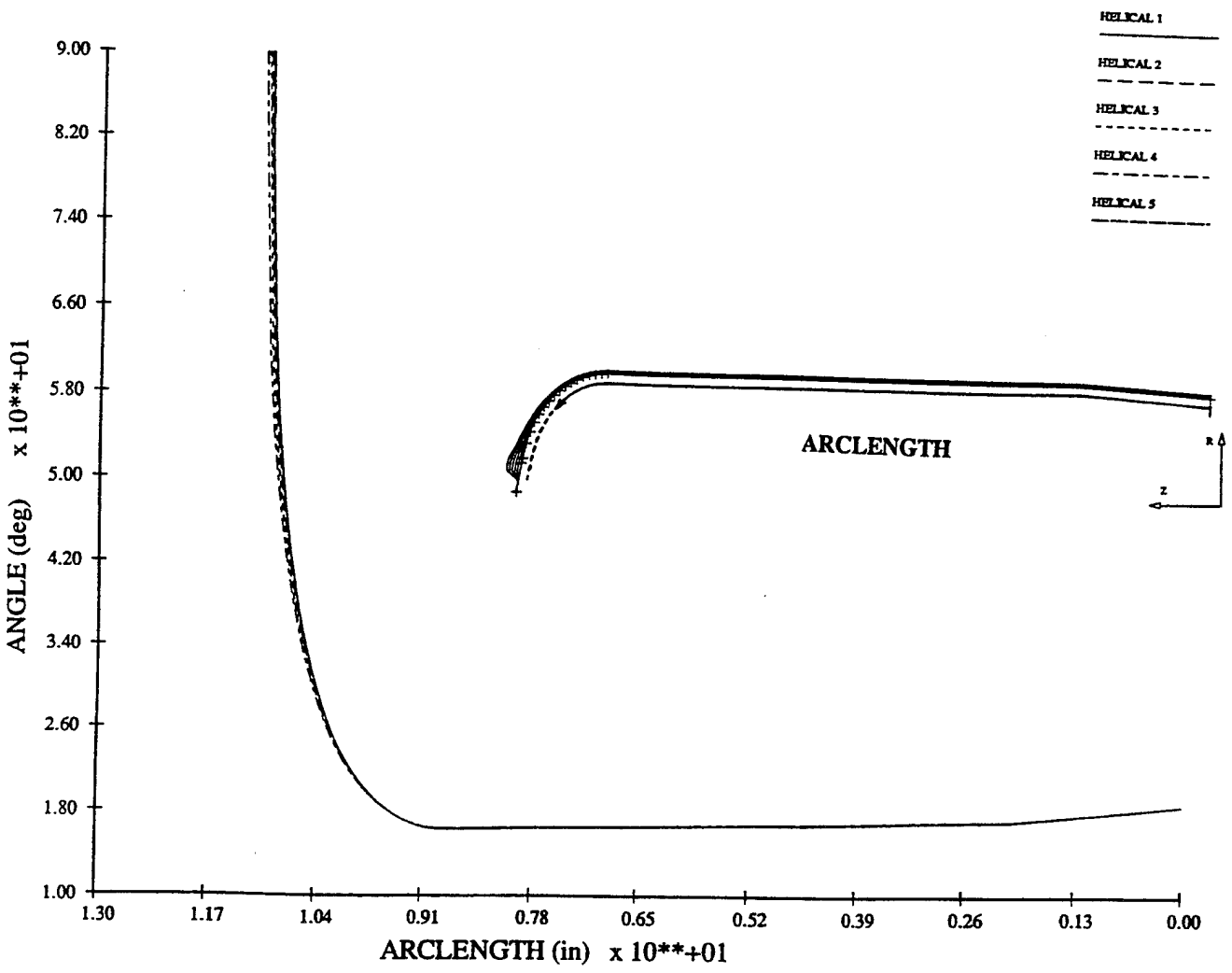

Figure 7. Winding angles (fiber orientations) vary along the arc-length of the composite case.

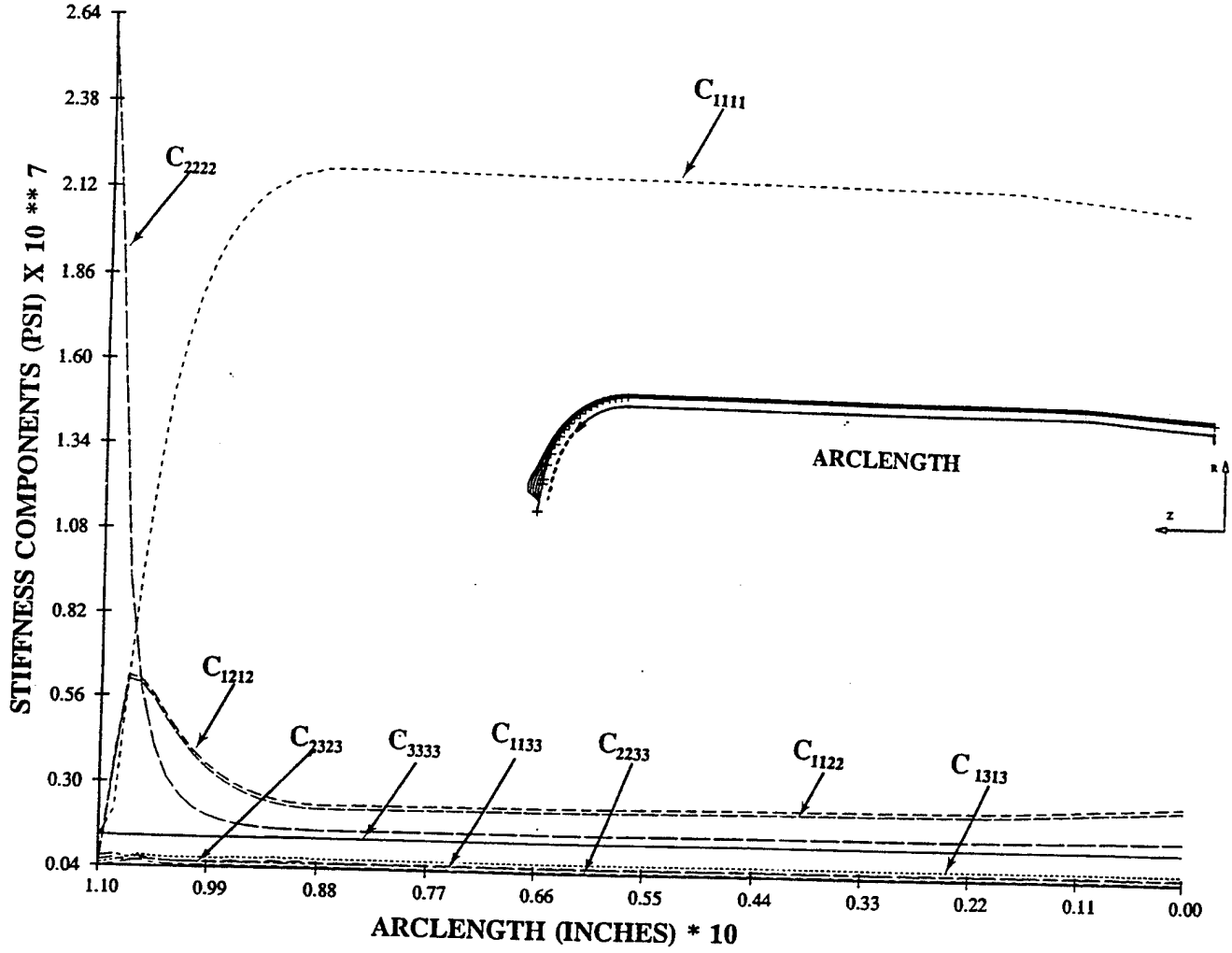

Figure 8. Stiffness components at the innermost layer vary along the arc-length.

5. CONCLUSIONS

Based on strain energy approaches and finite element techniques, an effective property model was developed to determine the properties of an arbitrarily shaped element with multi-material regions. The model is especially suitable for 3-D finite element application due to the accurate transverse shear properties. The effective material stiffness calculated by the model was compared to these by Chou's model. Significant differences in transverse shear properties were found for a four-ply cubic element. The comparison illustrated the lack of accuracy of currently available models. Effects of stacking sequence on transverse properties were identified and discussed in detail.

Having accurate transverse shear properties and the capability to model arbitrarily shaped elements are particularly important for finite element applications, especially for thick-section composites with near-net shape geometries subjected to complex loadings. A preprocessor was developed using the effective property model to generate properties for the finite element model. The preprocessor currently has capabilities to generate material properties for a finite element model for an axisymmetric filament-wound case and several other geometries of interest. The preprocessor is developed to be used with DYNA3D and ABAQUS finite element codes to perform dynamic analysis of composite structures with complex thick-section geometry.

6. REFERENCES

Chou, P. C., J. Carleone, and C. M. Hsu. "Elastic Constants of Layered Media." Journal of Composite Materials, vol. 6, 1972.

Christensen, R. M., and E. Zywicz. "A Three-Dimensional Constitutive Theory for Fiber Composite Laminates." Technical Report UCRL-100947, Lawrence Livermore Laboratory, 1989.

Enie, R. B., and R. R. Rizzo. "Three-Dimensional Laminate Moduli." Journal of Composite Materials, vol. 4, 1970.

Pagano, N. J. "Exact Moduli of Anisotropic Laminates in Composite Materials." Composite Materials, L. J. Broutman and R. H. Krock, eds. Mechanics of Composite Materials, G. P. Sendeckyj, ed., vol. 2, Academic Press, 1974.

Roy, A. K., and R. Y. Kim. "Experimental Determination of Transverse Shear Stiffness of a Thick Laminate." SEM Spring Conference on Experimental Mechanics, Cambridge, MA, 1989.

Roy, A. K., and S. W. Tsai. "Three-Dimensional Effective Moduii of Orthotropic and Symmetric Laminates." Journal of Applied Mechanics, vol. 59, 1992.

Sun, C. T., and S. Li. "Three-Dimensional Effective Elastic Constants for Thick Laminates." Journal of Composite Materials, vol. 22, 1988.

INTENTIONALLY LEFT BLANK.

NO. OF COPIES	ORGANIZATION
2	DEFENSE TECHNICAL INFO CTR ATTN DTIC DDA 8725 JOHN J KINGMAN RD STE 0944 FT BELVOIR VA 22060-6218
1	DIRECTOR US ARMY RESEARCH LAB ATTN AMSRL OP SD TA 2800 POWDER MILL RD ADELPHI MD 20783-1145
3	DIRECTOR US ARMY RESEARCH LAB ATTN AMSRL OP SD TL 2800 POWDER MILL RD ADELPHI MD 20783-1145
1	DIRECTOR US ARMY RESEARCH LAB ATTN AMSRL OP SD TP 2800 POWDER MILL RD ADELPHI MD 20783-1145
	ABERDEEN PROVING GROUND
5	DIR USARL ATTN AMSRL OP AP L (305)

NO. OF COPIES	ORGANIZATION
1	HQDA ATTN SARD TT DR F MILTON PENTAGON WASHINGTON DC 20310-0103
1	HQDA ATTN SARD TT MR J APPEL PENTAGON WASHINGTON DC 20310-0103
1	HQDA ATTN SARD TT MS C NASH PENTAGON WASHINGTON DC 20310-0103
1	HQDA ATTN SARD TR DR R CHAIT PENTAGON WASHINGTON DC 20310-0103
1	HQDA ATTN SARD TR MS K KOMINOS PENTAGON WASHINGTON DC 201310-0103
1	DIRECTOR US ARMY RESEARCH LABORATORY ATTN AMSRL CP CA D SNIDER 2800 POWDER MILL RD ADELPHI MD 20783
1	COMMANDER US ARMY ARDEC ATTN SMCAR FSE T GORA PICATINNY ARSENAL NJ 07806-5000
3	COMMANDER US ARMY ARDEC ATTN SMCAR TD R PRICE V LINDNER C SPINELLI PICATINNY ARSENAL NJ 07806-5000
1	COMMANDER US ARMY TACOM ATTN AMSTA JSK SAM GOODMAN WARREN MI 48397-5000

NO. OF COPIES	ORGANIZATION
1	COMMANDER US ARMY ARDEC ATTN F MCLAUGHLIN PICATINNY ARSENAL NJ 07806
5	COMMANDER US ARMY ARDEC ATTN SMCAR CCH T S MUSALLI P CHRISTIAN R CARR N KRASNOW PICATINNY ARSENAL NJ 07806-5000
1	COMMANDER US ARMY ARDEC ATTN SMCAR CCH V E FENNELL PICATINNY ARSENAL NJ 07806-5000
1	COMMANDER US ARMY ARDEC ATTN SMCAR CCH J DELORENZO PICATINNY ARSENAL NJ 07806-5000
2	COMMANDER US ARMY ARDEC ATTN SMCAR CC J HEDDERICH COL SINCLAIR PICATINNY ARSENAL NJ 07806-5000
1	COMMANDER US ARMY ARDEC ATTN SMCAR CCH P J LUTZ PICATINNY ARSENAL NJ 07806-5000
2	COMMANDER US ARMY ARDEC ATTN SMCAR FSA M D DEMELLA F DIORIO PICATINNY ARSENAL NJ 07806-5000
1	COMMANDER US ARMY ARDEC ATTN SMCAR FSA A WARNASH B MACHAK PICATINNY ARSENAL NJ 07806-5000

NO. OF COPIES	ORGANIZATION
8	DIRECTOR BENET LABORATORIES ATTN AMSTA CCB C KITCHENS J KEANE J BATTAGLIA J VASILAKIS G FFIAR V MONTVORI J WRZOCHALSKI R HASENBEIN WATERVLIET NY 12189
1	COMMANDER WATERVLIET ARSENAL ATTN SMCWV QAE Q C HOWD BLDG 44 WATERVLIET NY 12189-4050
1	COMMANDER WATERVLIET ARSENAL ATTN SMCWV SPM T MCCLOSKEY BLDG 25 3 WATERVLIET NY 12189-4050
1	COMMANDER WATERVLIET ARSENAL ATTN SMCWV QA QS K INSCO WATERVLIET NY 12189-4050
1	COMMANDER US ARMY ARDEC ATTN AMSMC PBM K PRODUCTION BASE MODERN ACTY PICATINNY ARSENAL NJ 07806-5000
1	COMMANDER US ARMY BELVOIR RD&E CTR ATTN STRBE JBC FT BELVOIR VA 22060-5606
1	US ARMY COLD REGIONS RESEARCH AND ENGINEERING LABORATORY ATTN P DUTTA 72 LYME RD HANOVER NH 03755
1	DIRECTOR US ARMY RESEARCH LABORATORY ATTN AMSRL WT L D WOODBURY 2800 POWDER MILL RD ADELPHI MD 20783-1145

NO. OF COPIES	ORGANIZATION
3	COMMANDER US ARMY MISSILE COMMAND ATTN AMSMI RD W MCCORKLE AMSMI RD ST P DOYLE AMSMI RD ST CN T VANDIVER REDSTONE ARSENAL AL 35898
2	US ARMY RESEARCH OFFICE ATTN A CROWSON J CHANDRA PO BOX 12211 RESEARCH TRIANGLE PARK NC 27709-2211
3	US ARMY RESEARCH OFFICE ENGINEERING SCIENCES DIV ATTN R SINGLETON G ANDERSON K IYER PO BOX 12211 RESEARCH TRIANGLE PARK NC 27709-2211
2	PROJECT MANAGER SADARM PICATINNY ARSENAL NJ 07806-5000
2	PROJECT MANAGER TANK MAIN ARMAMENT SYSTEMS ATTN SFAE AR TMA COL BREGARD K KIMKER PICATINNY ARSENAL NJ 07806-5000
1	PROJECT MANAGER TANK MAIN ARMAMENT SYSTEMS ATTN SFAE AR TMA MD R KOWALSKI PICATINNY ARSENAL NJ 07806-5000
2	PEO FIELD ARTILLERY SYSTEMS ATTN SFAE FAS PM D ADAMS T MCWILLIAMS PICATINNY ARSENAL NJ 07806-5000
1	PEO FIELD ARTILLERY SYSTEMS ATTN SFAE FAS PM H GOLDMAN PICATINNY ARSENAL NJ 07806
2	PROJECT MANAGER AFAS ATTN G DELCOCO J SHIELDS PICATINNY ARSENAL NJ 07806-5000

NO. OF COPIES	ORGANIZATION
2	NASA LANGLEY RESEARCH CTR MS 266 ATTN AMSRL VS W ELBER F BARTLETT JR HAMPTON VA 23681-0001
2	COMMANDER DARPA ATTN J KELLY B WILCOX 3701 N FAIRFAX DR ARLINGTON VA 22203-1714
2	COMMANDER WRIGHT PATTERSON AIR FORCE BASE ATTN WL FIV A MAYER DAYTON OH 45433
2	NAVAL SURFACE WARFARE CTR DAHLGREN DIV CODE G33 DAHLGREN VA 224488
1	NAVAL RESEARCH LABORATORY CODE 6383 ATTN I WOLOCK WASHINGTON DC 20375-5000
1	OFFICE OF NAVAL RESEARCH MECH DIV CODE 1132SM ATTN YAPA RAJAPAKSE ARLINGTON VA 22217
1	NAVAL ORDNANCE STATION ADVANCED SYSTEMS TECHNOLOGY BR ATTN D HOLMES CODE 2011 LOUISVILLE KY 40214-5245
1	DAVID TAYLOR RESEARCH CTR SHIP STRUCTURES AND PROTECTION DEPT ATTN J CORRADO CODE 1702 BETHESDA MD 20084
2	DAVID TAYLOR RESEARCH CTR ATTN R ROCKWELL W PHYILLAIER BETHESDA MD 20054-5000

NO. OF COPIES	ORGANIZATION
1	DEFENSE NUCLEAR AGENCY INNOVATIVE CONCEPTS DIV ATTN DR R ROHR 6801 TELEGRAPH RD ALEXANDRIA VA 22310-3398
1	DR FRANK SHOUP EXPEDITIONARY WARFARE DIV N85 2000 NAVY PENTAGON WASHINGTON DC 20350-2000
1	OFFICE OF NAVAL RESEARCH ATTN MR DAVID SIEGEL 351 800 N QUINCY ST ARLINGTON VA 22217-5660
1	NAVAL SURFACE WARFARE CTR ATTN CODE G30 JOSEPH H FRANCIS DAHLGREN VA 22448
3	NAVAL SURFACE WARFARE CTR ATTN CODE G33 JOHN FRAYSSE ROD HUBBARD GIL GRAFF DAHLGREN VA 22448
1	DEFENSE NUCLEAR AGENCY INNOVATIVE CONCEPTS DIV ATTN LTC JYUJI D HEWITT 6801 TELEGRAPH RD ALEXANDRIA VA 22448
1	CDR NAVAL SEA SYSTEMS CMD ATTN D LIESE 2531 JEFFERSON DAVIS HIGHWAY ARLINGTON VA 22242-5160
1	NAVAL SURFACE WARFARE ATTN CODE D4 MARY E LACY 17320 DAHLGREN RD DAHLGREN VA 22448
4	DIR LLNL ATTN R CHRISTENSEN S DETERESA F MAGNESS M FINGER PO BOX 808 LIVERMORE CA 94550

NO. OF COPIES	ORGANIZATION
1	DIR LANL ATTN D RABERN MEE 13 MS J 576 PO BOX 1633 LOS ALAMOS NM 87545
1	DIR LANL ATTN J REPPA MS F668 PO BOX 1663 LOS ALAMOS NM 87545
1	OAK RIDGE NATIONAL LABORATORY ATTN R M DAVIS PO BOX 2008 OAK RIDGE TN 37831-6195
4	DIR SANDIA NATIONAL LABORATORIES APPLIED MECHANICS DEPARTMENT ATTN DIVISION 8241 G BENEDETTI K PERANO D DAWSON P NIELAN PO BOX 969 LIVERMORE CA 94550-0096
1	BATTELLE ATTN C R HARGREAVES 505 KING AVE COLUMBUS OH 43201-2681
1	PACIFIC NORTHWEST LABORATORY ATTN M SMITH PO BOX 999 RICHLAND WA 99352
1	DIR LLNL ATTN M MURPHY PO BOX 808 L 282 LIVERMORE CA 94550
1	PURDUE UNIVERSITY SCHOOL OF AERO AND ASTRO ATTN C T SUN W LAFAYETTE IN 47907-1282
1	STANFORD UNIVERSITY DEPARTMENT OF AERONAUTICS AND AEROBALLISTICS DURANT BUILDING ATTN S TSAI STANFORD CA 94305

NO. OF COPIES	ORGANIZATION
1	UCLA MANE DEPT ENGR IV ATTN H THOMAS HAHN LOS ANGELES CA 90024-1597
2	U OF DAYTON RESEARCH INSTITUTE ATTN RAN Y KIM AJIT K ROY 300 COLLEGE PARK AVE DAYTON OH 45469-0168
2	UNIVERSITY OF DELAWARE CTR FOR COMPOSITE MATERIALS ATTN J GILLESPIE 201 SPENCER LABORATORY NEWARK DE 19716
1	THE UNIVERSITY OF TEXAS AT AUSTIN CENTER FOR ELECTROMECHANICS ATTN J PRICE 10100 BURNET RD AUSTIN TX 78758-4497
2	VIRGINIA POLYTECHNICAL INSTITUTE AND STATE UNIVERSITY DEPT OF ESM ATTN MICHAEL W HYER KENNETH L REIFSNIDER BLACKSBURG VA 24061-0219
1	AAI CORPORATION PO BOX 126 HUNT VALLEY MD 21030-0126
1	SAIC ATTN DAN DAKIN 2200 POWELL ST STE 1090 EMERYVILLE CA 94608
1	SAIC ATTN MILES PALMER 2109 AIR PARK RD S E ALBUQUERQUE NM 87106
1	SAIC ATTN ROBERT ACEBAL 1225 JOHNSON FERRY RD STE 100 MARIETTA GA 30068

NO. OF COPIES	ORGANIZATION
1	SAIC ATTN DR GEORGE CHRYSSOMALLIS 3800 W 80TH STREET STE 1090 BLOOMINGTON MN 55431
4	ALLIANT TECHSYSTEMS INC. ATTN C CANDLAND J BODE R BECKER K WARD 600 2ND ST NE HOPKINS MN 55343-8367
1	CUSTOM ANALYTICAL ENGINEERING SYSTEMS INC ATTN A ALEXANDER STAR ROUTE BOX 4A FLINTSTONE MD 21530
1	PROJECTILE TECHNOLOGY INC 515 GILES ST HAVRE DE GRACE MD 21078
1	ALLEN BOUTZ NOESIS INC 1110 N GLEBE RD STE 250 ARLINGTON VA 22201-4795
1	GENERAL DYNAMICS LAND SYSTEMS DIVISION ATTN D BARTLE PO BOX 1901 WARREN MI 48090
4	INSTITUTE FOR ADVANCED TECHNOLOGY ATTN T KIEHNE H FAIR P SULLIVAN I MCNAB 4030 2 W BRAKER LN AUSTIN TX 78759
1	INTERFEROMETRICS INC ATTN R LARRIVA VICE PRESIDENT 8150 LEESBURG PIKE VIENNA VA 22100

NO. OF COPIES	ORGANIZATION
2	OLIN CORPORATION FLINCHBAUGH DIV ATTN E STEINER B STEWART PO BOX 127 RED LION PA 17356
1	OLIN CORPORATION ATTN L WHITMORE 10101 9TH ST NORTH ST PETERSBURG FL 33702

NO. OF COPIES ORGANIZATION

ABERDEEN PROVING GROUND

55 DIR USARL
ATTN AMSRL SC
W MERMAGEN
C W STUREK
AMSRL SC S A MARK
AMSRL MA P L JOHNSON
AMSRL MA PD T CHOU
AMSRL MA PA D GRANVILLE
AMSRL MA MA G HAGNAUER
AMSRL SL B P DIETZ 328
AMSRL SL BA J WALBERT 1065
AMSRL SL BL D BELY 328
AMSRL SL I D HASKILL 1065
AMSRL WT P
A HORST 390A
E SCHMIDT 390A
AMSRL WT PA
T MINOR 390
D KOOKER 390A
AMSRL WT PB
P PLOSTINS 390
D LYON
AMSRL WT PC R FIFER 390A
AMSRL WT PD
B BURNS 390
W DRYSDALE 390
J BENDER 390
T ERLINE 390
D HOPKINS 390
S WILKERSON 390
R KASTE 390
L BURTON 390
J TZENG 390
R LIEB 390
G GAZONAS 390
C HOPPEL 390
AMSRL WT PD ALC
A ABRAHAMIAN
M BERMAN
A FRYDMAN
T LI
W MCINTOSH

NO. OF COPIES ORGANIZATION

ABERDEEN PROVING GROUND (CONTINUED)

AMSRL WT T W MORRISON 309
AMSRL WT TA
W GILLICH 390
W BRUCHEY 390
AMSRL WT TC
K KIMSEY 309
R COATES 309
W DE ROSSET 309
AMSRL WT TD
D DIETRICH 309
G RANDERS PEHRSON 309
A DAS GUPTA 309
J SANTIAGO 309
AMSRL WT W C MURPHY 120
AMSRL WT WA
H ROGERS 394
B MOORE 394
AMSRL WT WB
F BRANDON 120
W D AMICO 120
AMSRL WT WC J BORNSTEIN 120
AMSRL WT WD
A ZIELINSKI 120
J POWELL 120
AMSRL WT WE
J LACETERA 120
J THOMAS 394

INTENTIONALLY LEFT BLANK.

USER EVALUATION SHEET/CHANGE OF ADDRESS

This Laboratory undertakes a continuing effort to improve the quality of the reports it publishes. Your comments/answers to the items/questions below will aid us in our efforts.

1. ARL Report Number ARL-TR-1051 Date of Report April 1996

2. Date Report Received _____

3. Does this report satisfy a need? (Comment on purpose, related project, or other area of interest for which the report will be used.) _____

4. Specifically, how is the report being used? (Information source, design data, procedure, source of ideas, etc.) _____

5. Has the information in this report led to any quantitative savings as far as man-hours or dollars saved, operating costs avoided, or efficiencies achieved, etc? If so, please elaborate. _____

6. General Comments. What do you think should be changed to improve future reports? (Indicate changes to organization, technical content, format, etc.) _____

CURRENT ADDRESS

_____
Organization

_____
Name

_____
Street or P.O. Box No.

_____
City, State, Zip Code

7. If indicating a Change of Address or Address Correction, please provide the Current or Correct address above and the Old or Incorrect address below.

OLD ADDRESS

_____
Organization

_____
Name

_____
Street or P.O. Box No.

_____
City, State, Zip Code

(Remove this sheet, fold as indicated, tape closed, and mail.)
(DO NOT STAPLE)

DEPARTMENT OF THE ARMY

OFFICIAL BUSINESS

NO POSTAGE
NECESSARY
IF MAILED
IN THE
UNITED STATES

BUSINESS REPLY MAIL
FIRST CLASS PERMIT NO 0001,APG,MD

POSTAGE WILL BE PAID BY ADDRESSEE

DIRECTOR
U.S. ARMY RESEARCH LABORATORY
ATTN: AMSRL-WT-PD
ABERDEEN PROVING GROUND, MD 21005-5066